Depth Profiling of Stratified Layers using Variable Angle ATR

Robert A. Shick, Jack L. Koenig and Hatsuo Ishida

Department of Macromolecular Science

Case Western Reserve University

Cleveland, Ohio 44106

Abstract:

It is shown that variable angle attenuated total reflectance Fourier transform infrared spectroscopy is a viable technique to recover depth profile information on the molecular level. A number of controlled step profiles are measured to determine the limits of applicability for this method. Results obtained with a germanium and a KRS-5 prism are compared.

Introduction:

It is often desirable to have molecular information as a function of thickness within a sample. Such information can disclose the details of concentration gradients which would be of interest in a broad number of systems including polymer blends, polymer composites, and coatings. However, the recovery of the profile distribution is not straightforward. One method which will yield this information with proper treatment is variable angle attenuated total reflectance Fourier transform infrared spectroscopy (VA-ATR FTIR). In fact, any system which contains gradients as a function of depth could potentially benefit. This method allows the determination of concentration profiles as a function of depth within a sample without disrupting the sample. Currently, it is quite difficult to determine molecular gradient information in the micron size range, and an invasive technique is often used. However, even with proper treatment this method must be applied judiciously with proper regard to the restraints imposed by the

REPORT DOCUMENTATION PAGE

a REPORT SECURITY CLASSIFICATION None	1b. RESTRICTIVE MARKINGS None
2a SECURITY CLASSIFICATION AUTHORITY None	3. DISTRIBUTION / AVAILABILITY OF REPORT This document has been approved for public release and sale; its distribution is unlimited
2b DECLASSIFICATION / DOWNGRADING SCHEDULE None	
4. PERFORMING ORGANIZATION REPORT NUMBER(S) CWRU/DMS/TR - 44	5. MONITORING ORGANIZATION REPORT NUMBER(S)
6a NAME OF PERFORMING ORGANIZATION Case Western Reserve University 6b OFFICE SYMBOL (If applicable)	7a. NAME OF MONITORING ORGANIZATION Office of Naval Research
6c. ADDRESS (City, State, and ZIP Code) Department of Macromolecular Science Cleveland, Ohio 44106-1712	7b. ADDRESS (City, State, and ZIP Code) 800 North Quincy St. Arlington, VA 22217
8a NAME OF FUNDING / SPONSORING ORGANIZATION Office of Naval Research 8b OFFICE SYMBOL (If applicable)	9 PROCUREMENT INSTRUMENT IDENTIFICATION NUMBER
8c ADDRESS (City, State, and ZIP Code) 800 North Quincy Street Arlington, VA 22217	10 SOURCE OF FUNDING NUMBERS PROGRAM ELEMENT NO. / PROJECT NO. / TASK NO. / WORK UNIT ACCESSION NO

11 TITLE (Include Security Classification)
Depth Profiling of Stratified Layers using Variable Angle ATR

12 PERSONAL AUTHOR(S) Robert A. Shick, Jack L. Koenig, Hatsuo Ishida

13a TYPE OF REPORT	13b TIME COVERED	14 DATE OF REPORT (Year, Month, Day)	15. PAGE COUNT
Technical Report	FROM _____ TO _____		

16 SUPPLEMENTARY NOTATION
Submitted to "Applied Spectroscopy" 1/14/92

17 COSATI CODES			18 SUBJECT TERMS (Continue on reverse if necessary and identify by block number)
FIELD	GROUP	SUB-GROUP	

19 ABSTRACT (Continue on reverse if necessary and identify by block number)

It is shown that variable angle attenuated total reflectance Fourier transform infrared spectroscopy is a viable technique to recover depth profile information on the molecular level. A number of conrolled step profiles are measured to determine the limits of applicabiity for this method. Results obtained with a germanium and a KRS-5 prism are compared.

20 DISTRIBUTION / AVAILABILITY OF ABSTRACT ☒ UNCLASSIFIED/UNLIMITED ☐ SAME AS RPT. ☐ DTIC USERS	21. ABSTRACT SECURITY CLASSIFICATION unclassified
22a NAME OF RESPONSIBLE INDIVIDUAL Dr. Kenneth Wynne	22b. TELEPHONE (Include Area Code) (202) 696-4410 / 22c. OFFICE SYMBOL

OFFICE OF NAVAL RESEARCH

Contract N00014-92J-1047

Technical Report No. CWRU/DMS/TR-44

Depth Profiling of Stratified Layers Using Variable Angle ATR

by

Hatsuo Ishida, Jack L. Koenig, and Robert Shick

Department of Macromolecular Science
Case Western Reserve University
Cleveland, Ohio 44106-7202

January, 1992

Principal Investigator
Hatsuo Ishida
(216) 368-4285

optical constants of the materials involved. It is the intent of this paper to show experimentally that indeed this method can provide accurate profile information with well-known stratified layers. In addition, the limits with which this technique can be applied will be explored.

The governing principles of ATR have long been established. Harrick[1] was one of the pioneers in this field and he demonstrated that, above the critical angle required for internal reflection in a layered system, an evanescent wave is produced which decays exponentially from the surface of the material. Generally, it can be said that as the angle of incidence approaches the critical angle, the evanescent wave propagates to an increasing depth. In addition, this depth depends on the wavelength of incident radiation. A precise description of the field decay is known which includes the angle of incidence as an operable variable, as well as the refractive indices of the layers and the wavelength of the incident light. As the angle of incidence is changed, the field intensity is also changed, but any profile information at an individual depth is obscured by previous layers in an additive fashion. This difficulty may be overcome by applying inverse Laplace transform mathematics. Since infrared radiation is being employed, it is then possible to obtain vibrational spectroscopic information as a function of depth within the sample. It is the intent of this paper to illustrate the applicability of this method using well-known stratified layers. This will permit the evaluation of the experimental limits with which this technique can be reliably applied.

Theory:

The following is a review of Harrick's considerations[1]. For the attenuated total reflection experiment the evanescent wave decays in the following manner:

$$E = E_o\, e^{\frac{-2\pi z n_1}{\lambda}\sqrt{\left(\sin^2\theta - \left(\frac{n_2}{n_1}\right)^2\right)}} \qquad (1)$$

where the intensity, I, is equal to E^2. Here, n_2 refers to the refractive index of the sample and n_1 refers to the refractive index of the prism. The depth in the sample is "z," the wavelength is λ,

and the angle of incidence is θ. The absorptance for a single reflection, a, defined as 1-R, where R is the reflectance, is proportional to the intensity:

$$a = 1\text{-}R = \frac{n_2}{n_1 \cos\theta} \int_0^\infty \alpha E^2 \, dz \qquad (2)$$

where α is the extinction coefficient. However, the absorptivity profile is unknown, but this is proportional to the concentration profile of absorbing species. For rare absorbers:

$$a(\gamma) = k \int_0^\infty a(z) \, e^{-2\gamma z} \, dz \qquad (3)$$

Where here γ is the decay constant:

$$\gamma = \frac{2\pi n_1 \sqrt{\sin^2\theta - \left(\frac{n_2}{n_1}\right)^2}}{\lambda} \qquad (4)$$

This int ral is just the Laplace transform of a(γ) as was noted by Tompkins[2] and later by Hirschfeld[3]. What is meant by the statement of rare absorbers is that the field decay should be due principally to distance because the field actually decays due to distance and to absorption. If the absorption is too high, then the field decay due to absorption dominates over the spatial decay, and the field penetrates the sample to only a limited degree. The concentration profile, c(z), is of interest and is proportional to the inverse Laplace transform of a(γ):

$$c(z) = k\, a(z) = k\, \mathcal{L}^{-1}\{a(\gamma)\} \qquad (5)$$

This method requires a premeditated choice of concentration profile. Upon choosing a candidate profile, the specific parameters of the model are determined and the overall model is evaluated statistically. There have been other works involved with calculating depth profiles using VA-ATR by Popov et al.[4], Hobbs et al.[5], and most recently by Fina et al.[6] In addition to absorption spectroscopy, there has been an attempt to use these principles to recover the profile of fluorescing species as a function of depth using fluorescence data[7]. To this author's knowledge, however, there have been no experimental studies done on well known profiles which show the strengths and limitations of this technique. Therefore, it is the aim of this paper to show that the method indeed works and then to illustrate the range where it may be expected to work with unknown profiles by exploring the conditions where it works with known profiles.

Experimental:

Germanium and KRS-5 hemi-cylinders were obtained from Harrick Scientific. These hemi-cylinders were used in a variable angle attachment from Perkin Elmer. The incident angle was varied from the critical angle to a maximum of 64° with 2.5° increments. This allowed 16 individual spectra for the germanium and 10 for the KRS-5. The spectra were taken with a Bomem DA-3. Spectra were taken under vacuum (0.5 torr) and a liquid nitrogen cooled, narrow bandpass mercury-cadmium-telluride (MCT) detector was used with a specific detectivity D* of 2.1×10^{10} cm $Hz^{1/2}/W$. Happ-Genzel apodization was used and the resolution reported is after apodization. Typically, 2000 scans were co-added with a resolution of 4 cm^{-1} unless otherwise stated. Thin films of polymethylmethacrylate (PMMA) and polystyrene (PS) were deposited onto the hemi-cylinders from solution in spectrophotometric grade acetone obtained from Aldrich, and used as received. The PMMA, from Aldrich, was of medium molecular weight (M_w = 90,000) and was used as received. The PS, also from Aldrich, was of medium molecular weight (M_w = 45,000), and was also used as received. The thickness of the deposited films was controlled in the following manner. First, it was noted that for the dimensions of the hemi-cylinders, 200 µl could easily be held with surface tension. A solution of appropriate

concentration could be made which, when using 200 µl would, upon evaporation of the acetone, deposit a uniform film. The film thickness is calculated by considering the density of PMMA to be 1.17 g/cm^3 from Van Krevelen[8]. To assure the uniformity of the film, the evaporation was done in an acetone saturated environment, which served to slow the evaporation. Frequently, complete evaporation was achieved in 6 hours at room temperature. Next, the film was heated at 140 °C for 4 hours to assure that all traces of the acetone had been completely removed. Films were prepared with thicknesses between 0.5 and 3 µm.

Results and Discussion:

The reciprocal of γ, the reciprocal of eqn. 4, is often used as a characteristic depth of penetration. However, it is really a decay constant, and its value as a function of angle is shown in Figure 1 for a germanium prism (refractive index, RI, of 4.00) considering a few different frequencies. Normal incidence to the sample is considered 0° incidence angle. What is important is that, as the angle is decreased, γ becomes smaller until it goes to zero at the critical angle. This means that at small angles the evanescent wave is penetrating very deeply into the sample, yielding information both close to the prism and far into the sample. As the incident angle is increased, γ also increases, indicating that the wave is becoming more concentrated near the prism. Therefore, as the angle is progressively increased, the spectral information is being successively excluded from the deeper regions and is being concentrated close to the prism. In order to have information directly in the vicinity of the prism surface, γ would have to become very large. However, this is not the case. From the figure it is obvious that γ reaches a plateau value at high angles. This indicates that there is some minimum thickness that can be probed as well as a maximum, and that both the minimum and maximum will be frequency dependent.

The primary goal of this paper is to show that depth profiling is feasible using VA-ATR. The experimental configuration used in this paper is shown in Figure 2, where a 0.5 µm PMMA layer has been coated onto a germanium hemi-cylinder. Because there is no general solution to an inverse Laplace transform, a general form must be assumed. At this point, a step profile will

be assumed, but the thickness, t_{PMMA}, will be determined from the data, in addition to the minimum thickness, t_{min}, which can be estimated. For a step profile, the analytic solution of the Laplace transform is as follows:

$$a_{PMMA}(s) = \mathcal{L}\{a_{PMMA}(z)\} = \frac{k}{\cos\theta} \frac{e^{-t_{min}s} - e^{-t_{PMMA}s}}{s} \qquad (6)$$

where $s = 2\gamma$, and the $\cos\theta$ term is frequently referred to as the area correction term. Therefore, the numerical fitting is done in the Laplace plane and the parameters then relate to the inverse Laplace plane which is distance, z, for this case. So, the spectra are recorded as a function of angle, and then the absorptance, $a(\theta)$, is transformed to a function of s, a(s) and then fit to eqn. 6. The non-linear least squares estimation is done using a Simplex algorithm which is a component of a statistics package, Systat, from Systat Inc.

The results of this estimation for the carboxylic ester region of the PMMA are shown in Figure 3. It is expected that if this method is working correctly that the same estimate of thickness will be obtained regardless of frequency. It is quite encouraging that this is indeed what is observed. The same estimate of thickness, about 0.5 μm, is obtained for all of the peaks in the carboxylic ester region. The dashed line is not a best fit line of the estimates, rather it is the thickness which was calculated from the solution deposition. The VA-ATR technique determined an estimate for the PMMA thickness completely independently. There is very good agreement between the deposited thickness and that estimated by the VA-ATR technique. This is also very reproducible. If some of the spectral parameters such as the baseline, resolution, aperture, or polarization are changed there is a variation of about 5%. Because the actual thickness is known in this instance, it is possible to say that the estimates are in very good agreement, in other words, that the actual error is very small. However, for cases where the actual thickness is not known, the case for an unknown sample, another method is required to assess the error. To accomplish this, all of the error of the non-linear fitting is distributed to each of the estimated parameters depending upon its relative impact on the model, through the magnitude of the second derivative matrix. The statistics package used for analysis has this

capability. Figure 4 shows the same estimation, but with the statistical error bars attached. The statistical error significantly over-estimates the actual error for every case. Therefore, if this were an unknown sample, the estimate with the lowest statistical error would be used, namely the peak at 1192 cm^{-1} would be used because it has an error of about 10%, the lowest shown. It should be emphasized that the only explicit assumptions made were that the PMMA was a step profile of arbitrary thickness and that the real part of the refractive index of PMMA was 1.5.

The preceding result was for a layer of PMMA on germanium with air as a backing, but the same result should be obtained regardless of what is behind the PMMA. Figure 5 depicts the situation where a 0.5 mm layer of PMMA is coated onto germanium with a mineral oil, Nujol, behind the PMMA. As can be seen from the figure, there is no effect of a nujol overlayer on the estimation of the thickness of the PMMA.

At this point, it was interesting to consider the possibility of reducing the statistical error by controlling the polarization of the radiation incident on the sample. Using the optical convention that light in the reflecting plane is parallel polarized and that light perpendicular to the reflecting plane is perpendicular polarized, then the initial evanescent field strength is as follows[1]:

$$E_{\parallel} = \left\{ \frac{4\left(\sin^2\theta - \left(\frac{n_2}{n_1}\right)^2\right)\cos^2\theta + 4\sin^2\theta\cos^2\theta}{\left(1 - \left(\frac{n_2}{n_1}\right)^2\right)\left[\left(1 + \left(\frac{n_2}{n_1}\right)^2\right)\sin^2\theta - \left(\frac{n_2}{n_1}\right)^2\right]} \right\}^{\frac{1}{2}} \tag{7}$$

$$E_{\perp} = \frac{2\cos\theta}{\left(1 - \left(\frac{n_2}{n_1}\right)^2\right)^{\frac{1}{2}}} \tag{8}$$

The most important attribute of eqns. 7 and 8 is that they are different. The evanescent field should decay the same independent of polarization, but the initial field strength is not. Because of this, it was desirable to perform the same experiments but maintaining polarization. For this a wire grid polarizer on KRS-5 was used with a germanium prism. Unfortunately, the signal-to-

noise ratio was too low to perform the analysis. Therefore, at this point, the prism material was changed to KRS-5, with a refractive index of 2.37. There is significantly better throughput due to the lower refractive index. In addition to maintaining polarization, it is also interesting to vary the thickness of the PMMA layer to determine the experimental limits of the technique. Figure 6 depicts the results obtained for a 0.55 μm layer of PMMA deposited onto KRS-5. It is evident that the overall statistical error is somewhat larger than for germanium, but the lower values are quite acceptable. The statistical error is still seen to over-estimate the actual error, but the estimates are systematically higher than the actual thickness. This indicates that this is close to the lower limit of thickness which can be effectively measured.

The thickness of the PMMA layer is increased to 0.8 μm and the results are shown in Figure 7. Here, it is evident that there is very close estimation of the actual thickness. The results shown in Figure 8 are for a 1.05 μm layer of PMMA. Again the estimates are very close to the actual thickness. If the thickness is increased further to 1.4, 2 or 3 μm, the PMMA layer can no longer be estimated. Therefore, 1.05 μm is very close to the upper limit which may be estimated using this technique. It is important to remember that the depth profiling is not limited to the carboxylic ester region. Figure 9 shows the thickness estimation for 0.8 μm PMMA on KRS-5 for the spectral "fingerprint" region, from 1800 to 1100 cm^{-1}. Actually, the lower frequency absorptions give somewhat better estimates for thick films because they are penetrating deeper into the sample. Likewise, higher frequency absorptions give better estimates for thinner films. Indeed, if the C-H stretching region (just under 3000 cm^{-1}) is examined it is possible to conclude that the PMMA film begins very close to the prism, within 0.01 μm, and then from the fingerprint region it is possible to determine how far it extends. Thus, the range which may be safely probed using KRS-5 is from about 0.6 to about 1.0 μm using the fingerprint region, however, the lower range may be extended using the C-H stretching region.

It is interesting to explore the effects of different experimental conditions on the statistical error. Because a 0.8 μm film of PMMA on KRS-5 is safely within the measurement range, it will be used to observe these effects. Recall figure 7, here the spectra were taken with a

1.0 mm aperture, with polarization, and with 8 cm^{-1} resolution. The effects of removing the polarizer are shown in Figure 10. The error on the estimates becomes slightly worse, but basically the results are the same as with the polarizer. This is probably no surprise since if the data had self polarization effects either from the attachment or sample, the presence of the polarizer would be of no value. Therefore, it seems that the loss in energy throughput from the polarizer is not compensated by any added advantage. Accordingly, the use of a polarizer is ill-advised for depth profiling.

The effects of reducing the aperture from 1.0 to 0.5 mm are shown in Figure 11. There is a significant reduction in the statistical error in this figure. This is somewhat expected because angular accuracy is at the heart of this technique. An aperture of 0.5 mm is at the lower limit of the current experimental configuration. The effects of changing the spectral resolution to 4 cm^{-1} is shown in Figure 12. The error is seen to be slightly higher, which is expected because there is a trade-off for spectral accuracy and depth accuracy. The depth accuracy is adversely affected by a reduced signal-to-noise ratio, which is the result of increased spectral accuracy, everything else being equal. So the best conditions are as small an aperture as possible (0.5 mm for our configuration), no polarization, and moderate spectral resolution. In addition, the more data there is, the better the overall fit, and there are 16 angles for germanium as opposed to 10 for KRS-5, due to the lower critical angle of germanium. Therefore, there is an inherently better accuracy for the germanium prism, although there is a smaller range of depths which may be probed. The range for germanium with PMMA has not been precisely determined, but the technique failed to yield the thickness of a 0.75 μm layer, so this is above the upper limit. It was shown in figure 2 that a 0.5 μm layer could be estimated, and it appears from the t_{min} estimates that the lower limit should be around 0.3 μm. Again, the presence of a lower limit is somewhat nebulous because it is targeted for the "fingerprint" region, and using the C-H stretching region there is practically no lower limit, although the upper limit for this region has yet to be determined.

It has been shown that the characteristics of single step profile could be recovered using the VA-ATR technique. Now, it is interesting to see if a double step profile can be determined. This is a more challenging system than the ones previously investigated. For this sample, a 0.5 μm layer was deposited onto a germanium hemi-cylinder, as before. A very thick layer of PS, about 100 μm, was placed on top of the PMMA, and heated to 140°C. This temperature is above the glass transition of both the PS and the PMMA, and it assures good optical contact between the layers. It is well-known that PMMA and PS are incompatible, therefore it is expected that a clean interface will develop between the polymers at 0.5 μm from the surface of the germanium. In this sample, there are two profiles to consider. By examining regions of the spectra from the PMMA, it is possible to determine how far the PMMA extends. In addition, by examining regions of the spectra due to PS it is possible to determine how far it is until the PS begins. The infrared spectra for these two pure polymers are shown in Figure 13. Because the PMMA layer is directly next to the germanium, its spectra will be much more intense than that for the PS. Therefore, it is possible to use the carboxylic ester region for PMMA as before, even though there is a slight overlap with the PS peaks. However, it is very important to choose a completely non-overlapping peak for the PS. The ring-hydrogen bending mode at 1028 cm^{-1} is quite free from overlap. The VA-ATR results are shown in Figure 14. From this figure it can be seen that the PMMA extends to about 0.5 μm according to the data from the carboxylic ester region of the PMMA. In addition, the PS layer does not begin until about 0.5 μm, in very good agreement with what was expected.

Thus far, it has been shown that the VA-ATR technique can be used to determine one and two layer profiles relatively accurately, but that it is necessary to make some kind of assumption as to the overall nature of the distribution. This assumption cannot be removed. Therefore, another approach has been used to overcome this restriction. Instead of an abrupt step profile, it is possible to replace the unknown distribution with a sum of step profiles. In principle, this should allow enough flexibility to determine any unknown profile. This approach can be applied to the data shown in Figure 11 to test how well this idea will work. Recall that this is a 0.8 μm

layer of PMMA on KRS-5, and this data was chosen because it offered the lowest statistical error of the various experimental conditions. Knowing that the best error which was achieved was about 10%, it is undesirable to make the spectral slices below the error level. In addition, the effective range for KRS-5 was determined to be 0.6 to 1.0 μm. Therefore, a sum of four individual step profiles will be used, however their distances will be fixed to 0.1 μm increments and the absorption for each of those increments will be determined. This allows one to obtain, in principle, a complete spectra for each individual increment. The Laplace transform will then be:

$$a(s) = \frac{\{k_1(e^{-0.6\,s} - e^{-0.7\,s}) + k_2(e^{-0.7\,s} - e^{-0.8\,s}) + k_3(e^{-0.8\,s} - e^{-0.9\,s}) + k_4(e^{-0.9\,s} - e^{-1.0\,s})\}}{s \cos\theta} \qquad (9)$$

The results are shown in Figure 15. This is a three-dimensional representation of spectral slicing, and it is in agreement with the previous results. The PMMA is present until the 0.8 to 0.9 μm layer, and which point it ends, and there is no PMMA past 0.9 μm. There is some sacrifice in spatial accuracy because more of the degrees of freedom are being used to determine the overall profile, which previously had been assumed. The advantage of this approach is that in principle a complete spectra may be obtained for each depth interval. This is indeed observed for the PMMA, where the spectra in the carboxylic ester region are maintained until the PMMA layer ends. This method is quite flexible, and is limited only by the number of data and their accuracy. Thus, with an improved statistical error, even thinner increments may be adopted.

There are a number of implicit assumptions in this method. For the most part, only the real part of the refractive index was assumed to dominate the evanescent wave decay, and this is a necessary assumption to make depth profiling tractable. This is mostly true for relatively weak absorptions. However, it is possible to completely simulate all of the experiments which were presented knowing the optical constants of the materials. This removes any experimental errors which are inherently present in any empirical study, and lends credence to this method from a more fundamental point of view. The limits which were observed experimentally were found to agree quite closely with those found from purely theoretical considerations, in other words, when

the implicit assumptions were no longer valid. The complete theoretical argument is somewhat lengthy, and is the subject of a separate paper[9].

Conclusions:

It has been shown that depth profile information using a variable angle ATR technique is in very good experimental agreement with known values for well controlled stratified layers. The statistical error calculated for all cases far exceeded the actual experimental error. Therefore, when applying this technique on unknown samples it is reasonable to expect errors of approximately 10%. It is possible to accurately probe between 0.6 and 1.0 μm using a KRS hemi-cylinder in the spectral "fingerprint" region. There is essentially no lower limit when using the C-H stretching region. It is possible to probe smaller distances more accurately using a germanium hemi-cylinder.

Acknowledgment:

This work was supported in part by a grant from the Office of Naval Research.

References:

1 N.J. Harrick, "Internal Reflection Spectroscopy," Interscience, Wiley, New York, 1967.

2 H.G. Tompkins, *Appl. Spectrosc.*, **28**, 335 (1974).

3 T. Hirschfeld, *Appl. Spectrosc.*, **31**, 289 (1977).

4 V.Y. Popov and V.V. Lavrent'ev, translated from *Zhur. Prikl.Spektrosk.*, **32**, 336 (1980).

5 J.P. Hobbs, C.S. Sung, K. Krishnan, and S. Hill, *Macromolecules*, **16**, 193 (1983).

6 L. Fina and G. Chen, *Vibrational Spectrosc.*, **1**, 353 (1991).

7 W.M. Reichert, P.A. Suci, J.T. Ives, and J.D. Andrade, *Appl. Spectrosc.*, **41**, 503 (1987).

8 D.W. Van Krevelen, "Properties of Polymers," Elsevier, New York, 1976.

9 R. Shick and H. Ishida, *Appl. Spectrosc.*, submitted February 1992.

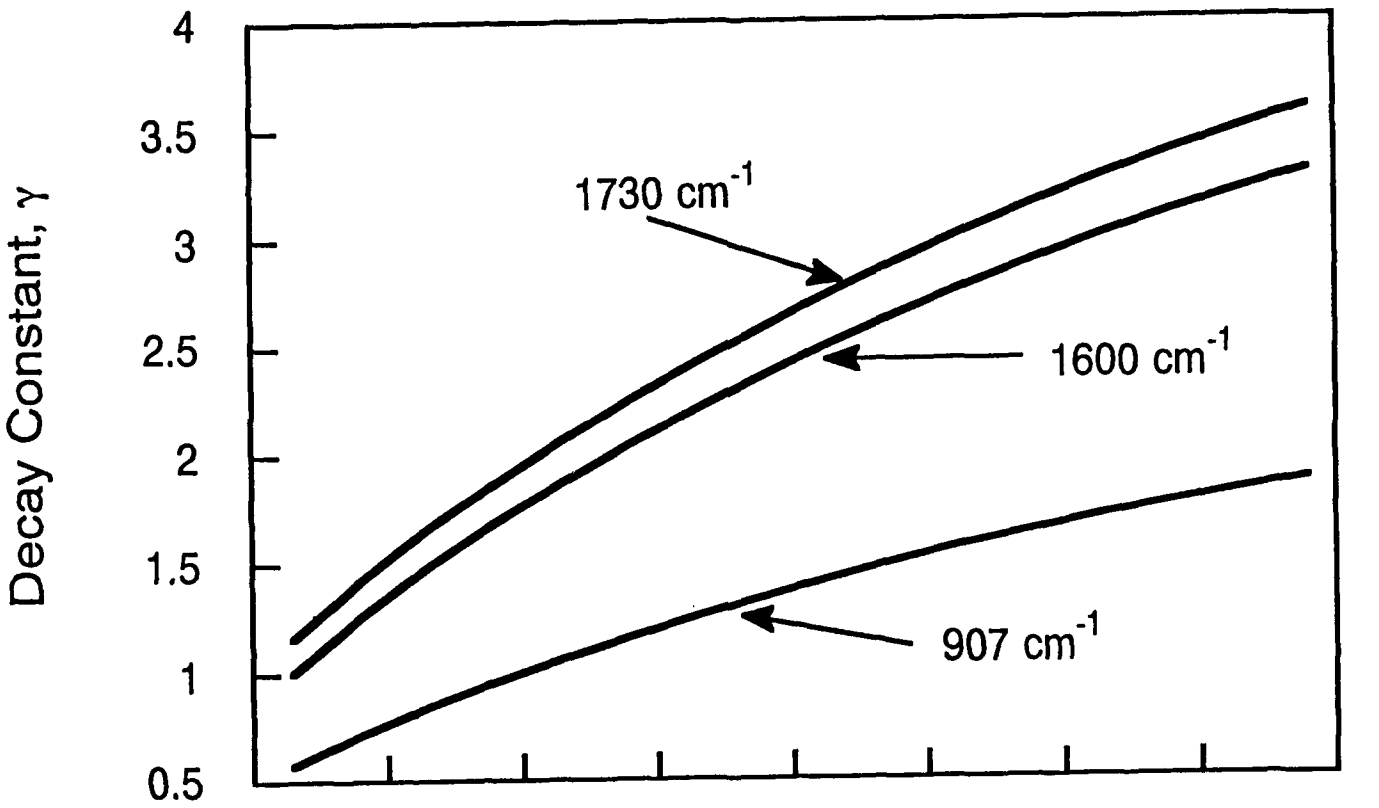

Shick et al. Figure 1

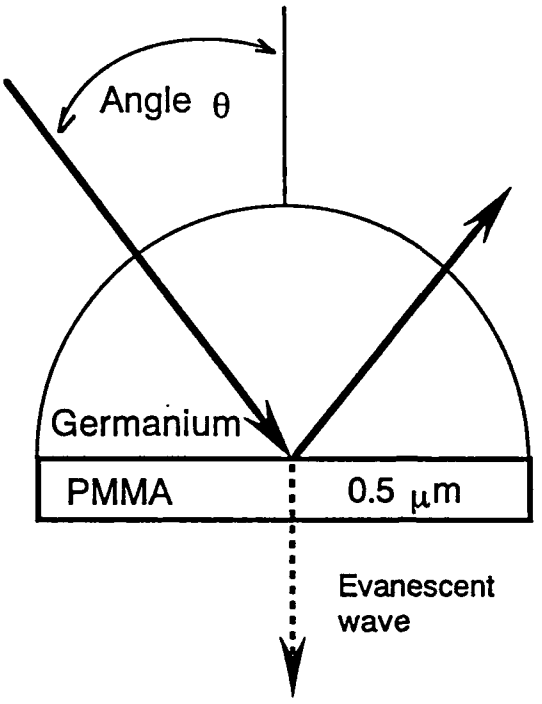

Shick et al. Figure 2

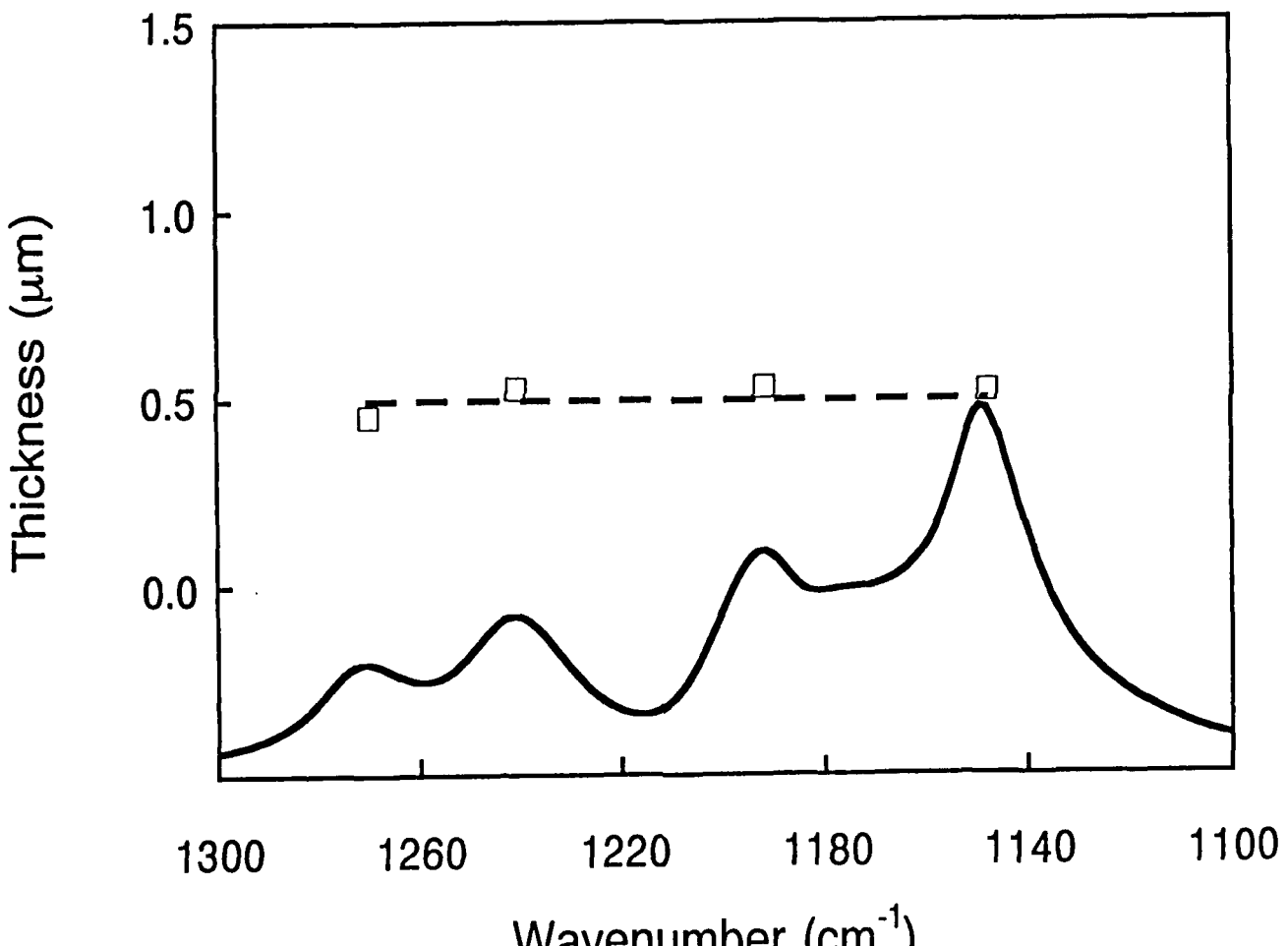
1.5
1.0
0.5
0.0
Thickness (μm)
1300
1260
1220
1180
1140
1100
Wavenumber (cm-1)

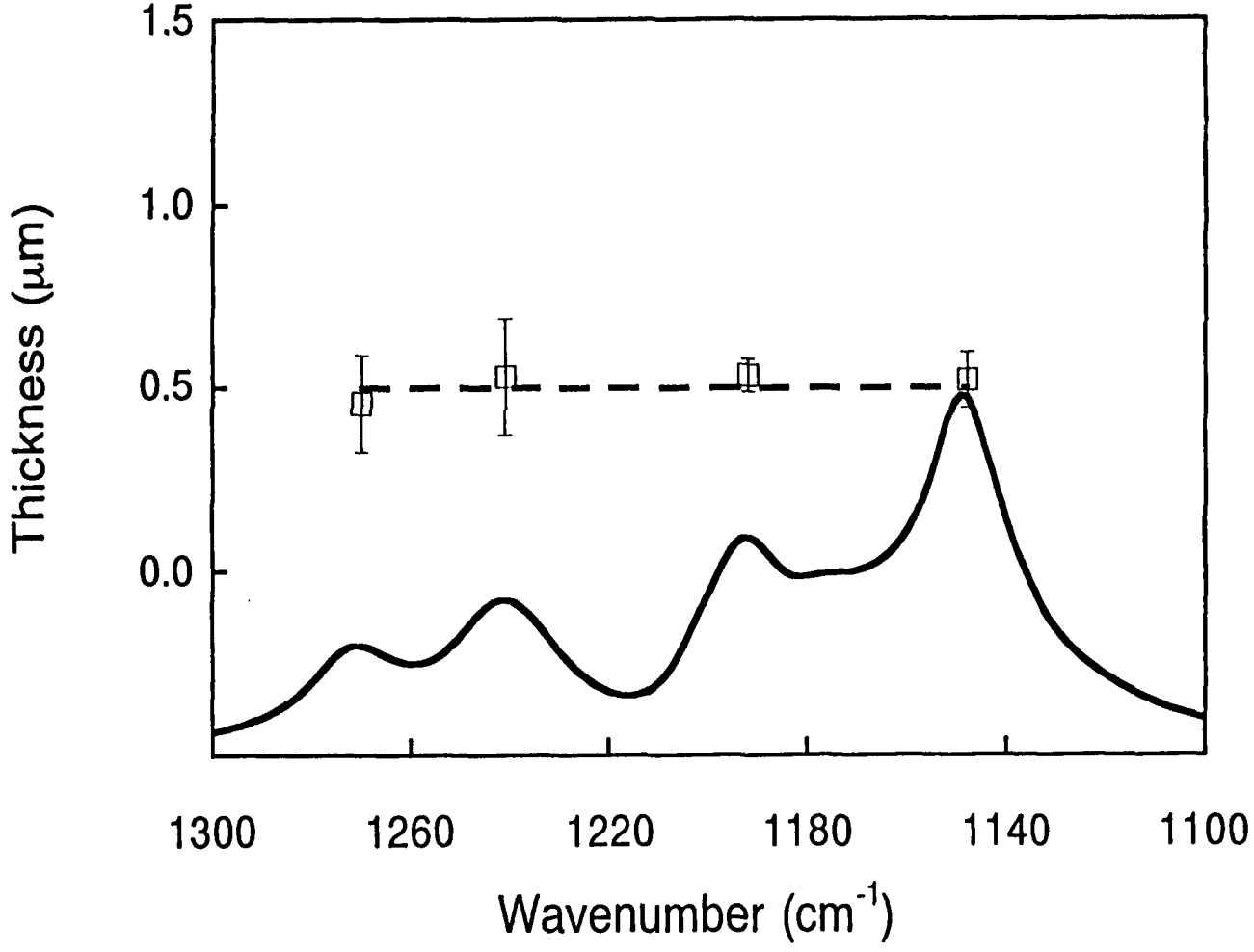
1.5
1.0
0.5
0.0
Thickness (μm)
1300
1260
1220
1180
1140
1100
Wavenumber (cm-1)

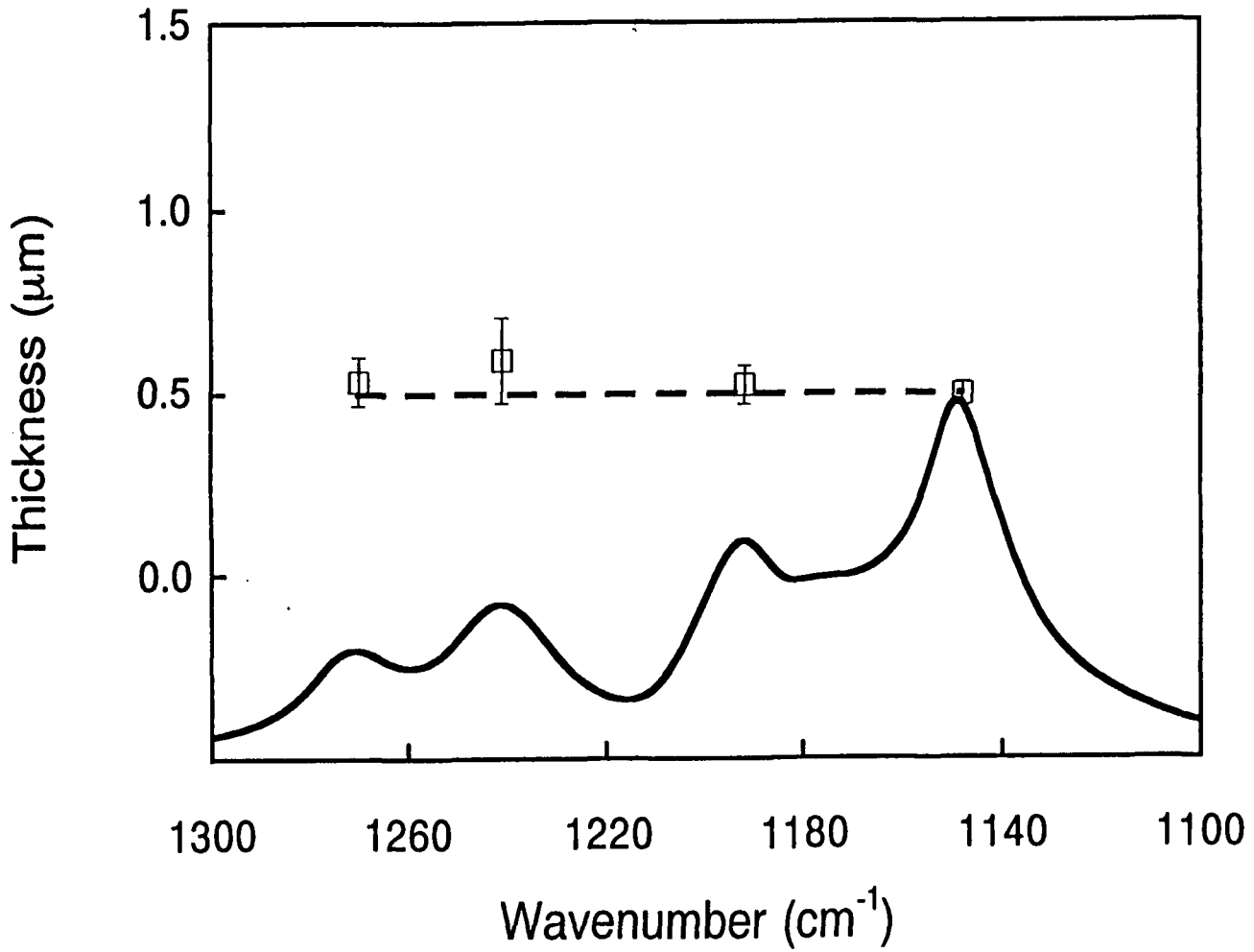
1.5
1.0
0.5
0.0
Thickness (μm)
1300
1260
1220
1180
1140
1100
Wavenumber (cm-1)

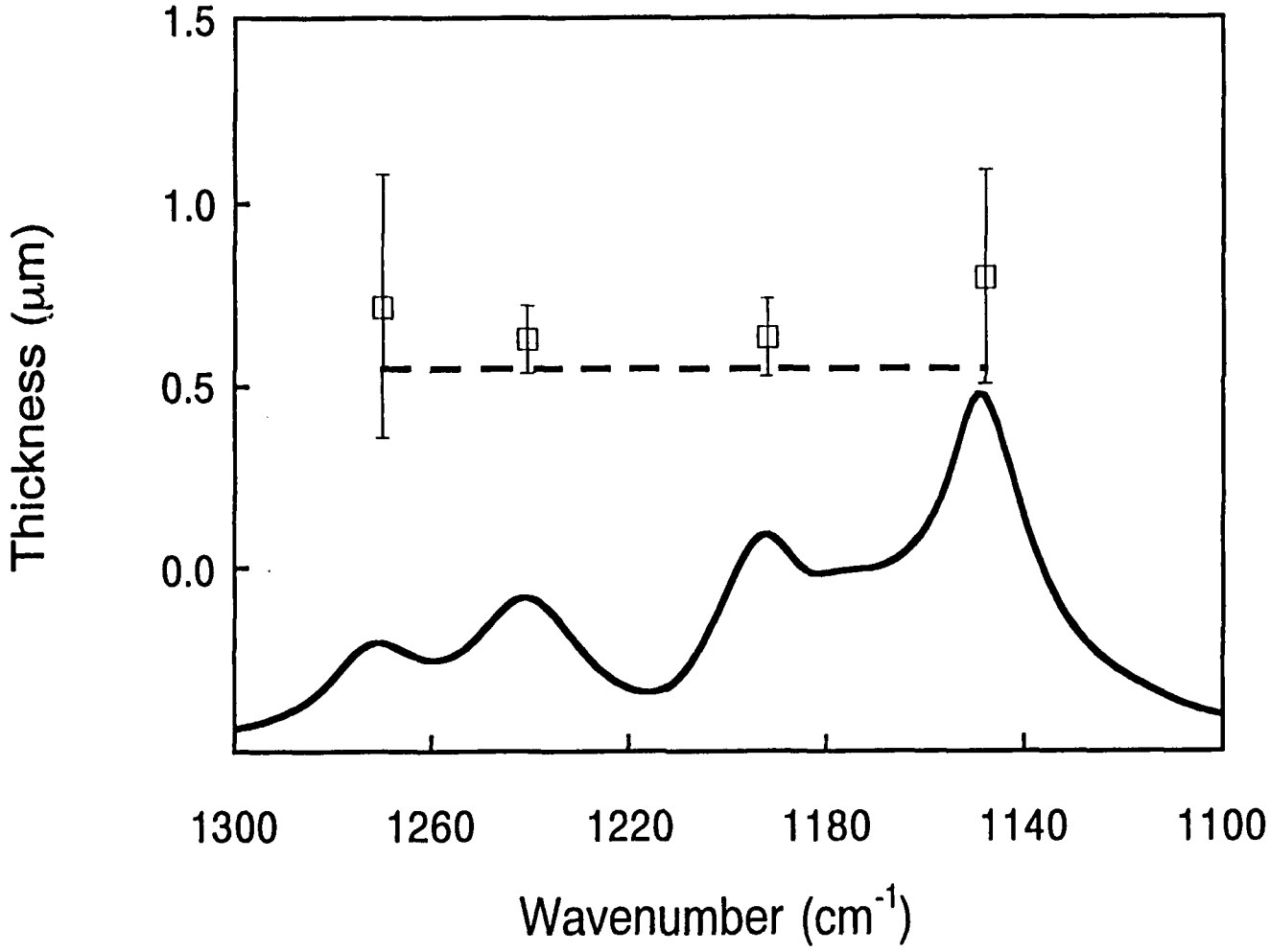
1.5
1.0
0.5
0.0
Thickness (μm)
1300
1260
1220
1180
1140
1100
Wavenumber (cm-1)

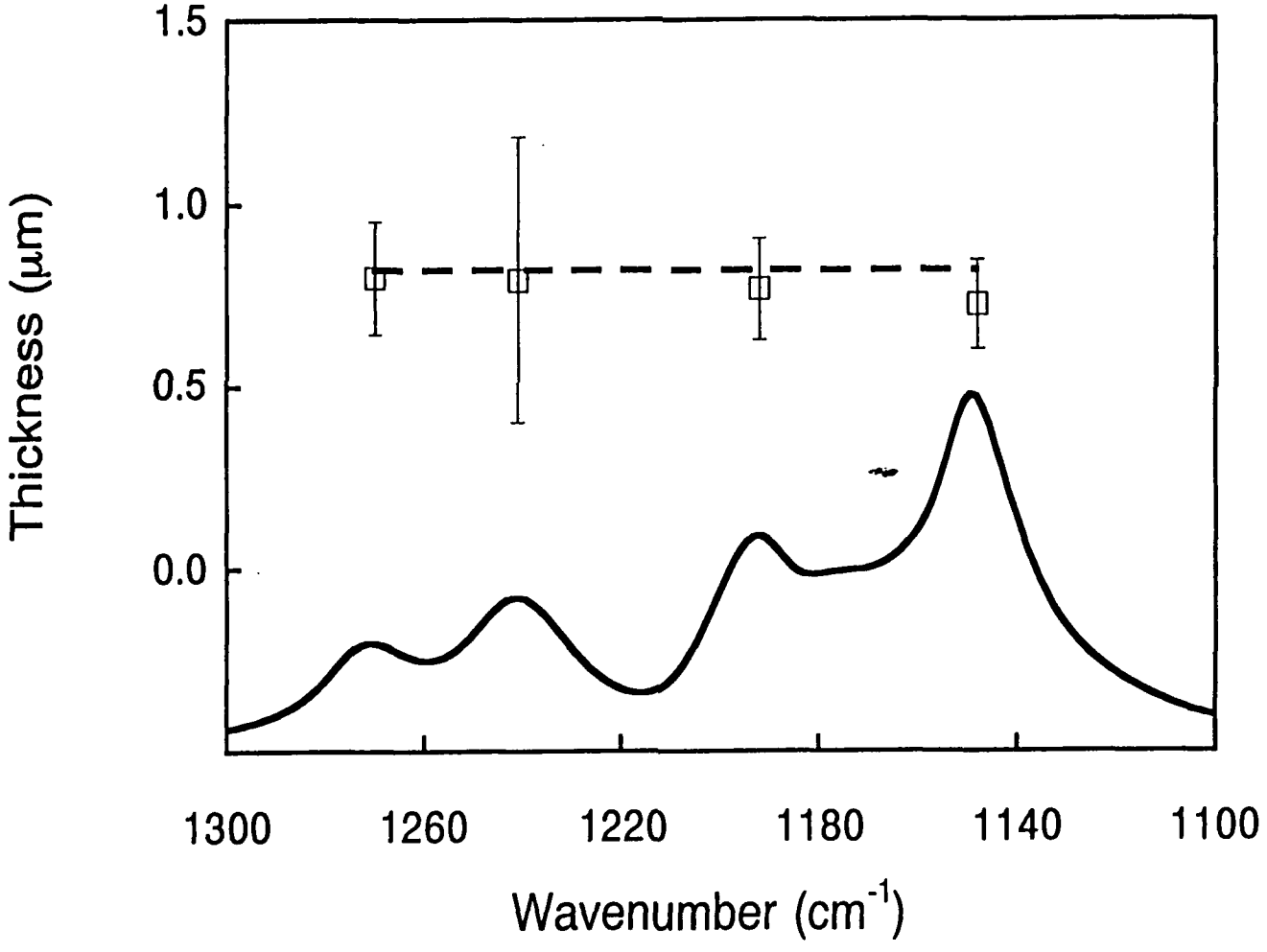
1.5
1.0
0.5
0.0
Thickness (μm)
1300
1260
1220
1180
1140
1100
Wavenumber (cm-1)

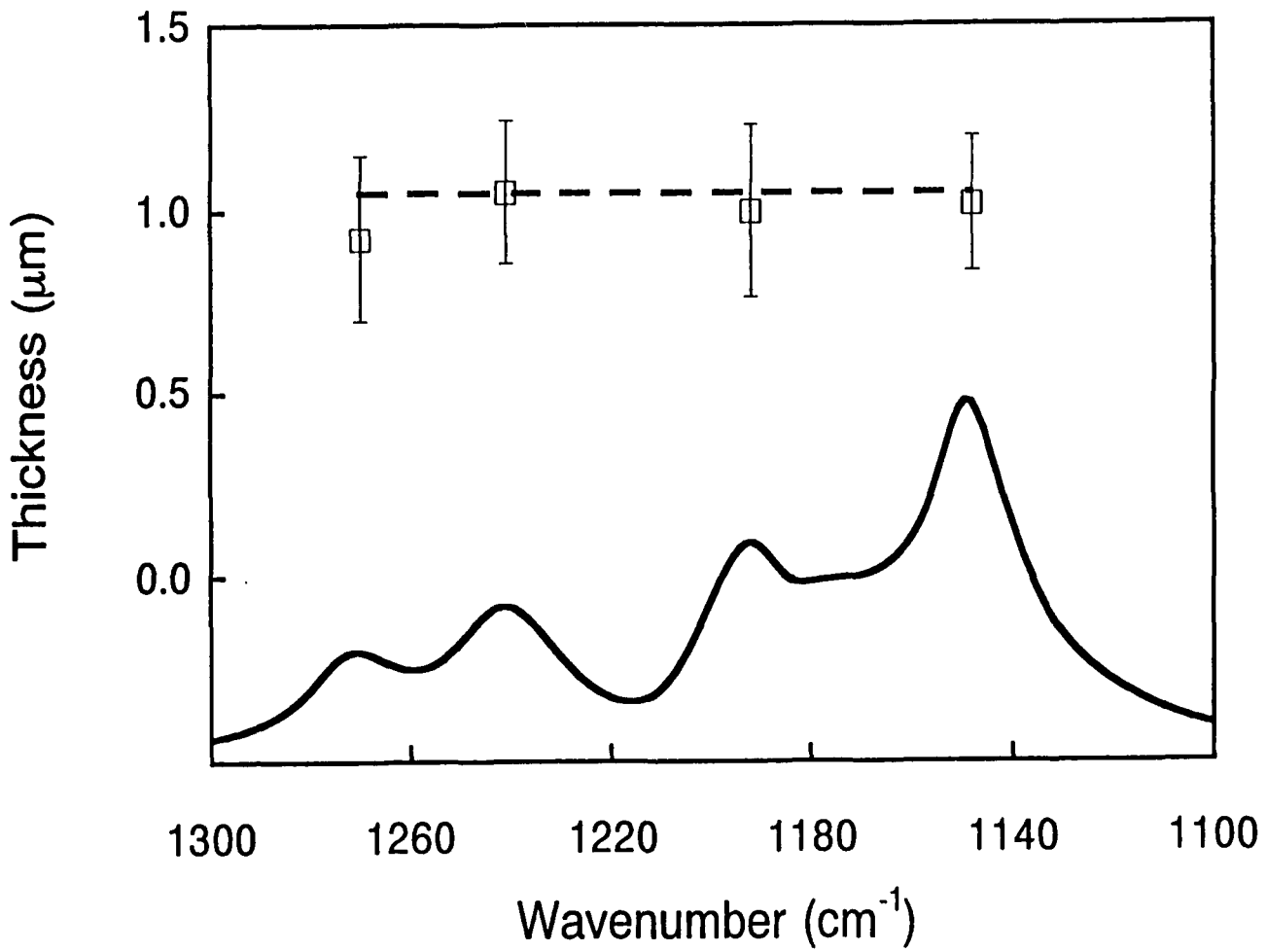
1.5
1.0
0.5
0.0
Thickness (μm)
1300
1260
1220
1180
1140
1100
Wavenumber (cm-1)

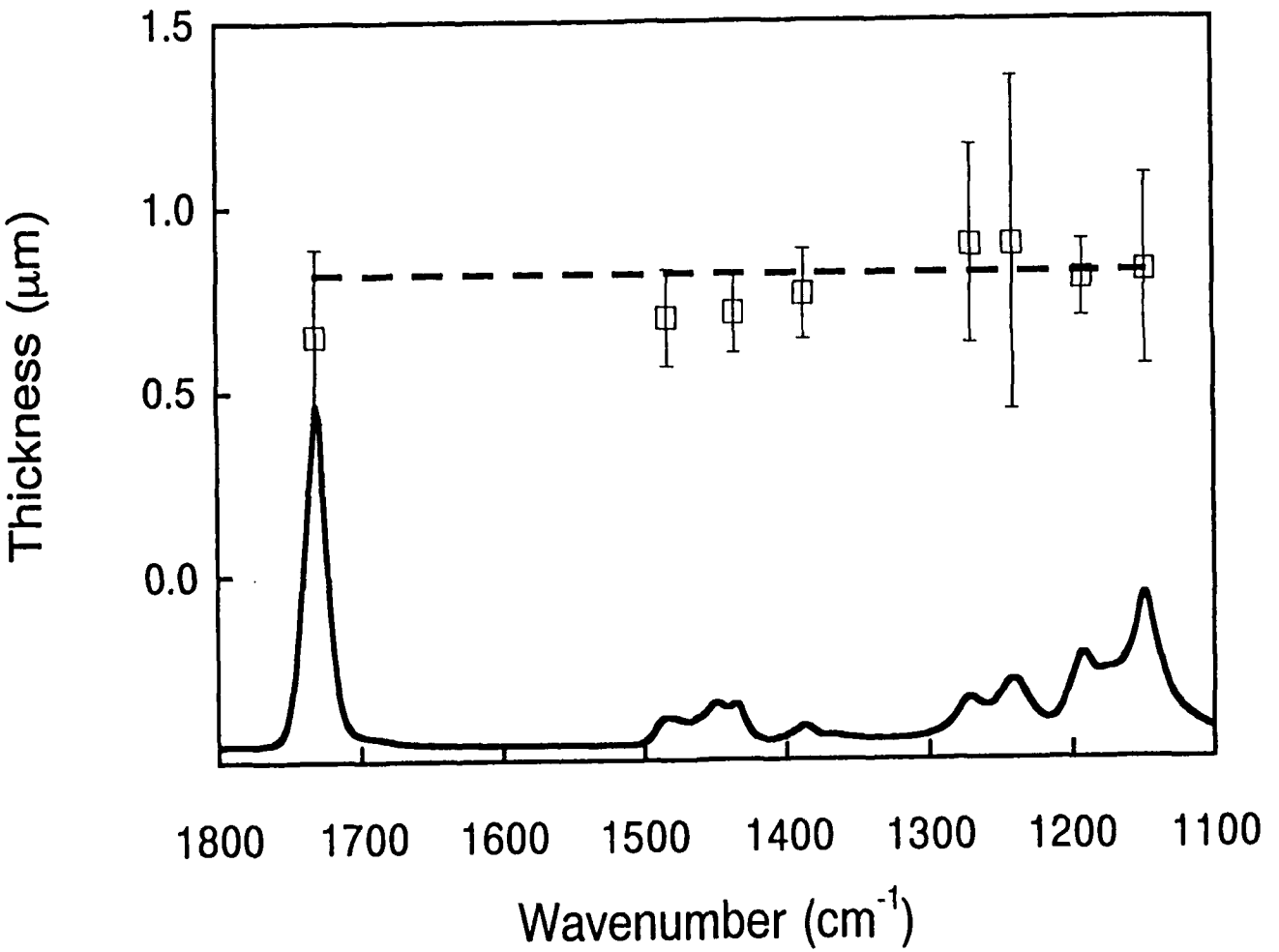
1.5
1.0
0.5
0.0
Thickness (μm)
1800
1700
1600
1500
1400
1300
1200
1100
Wavenumber (cm-1)

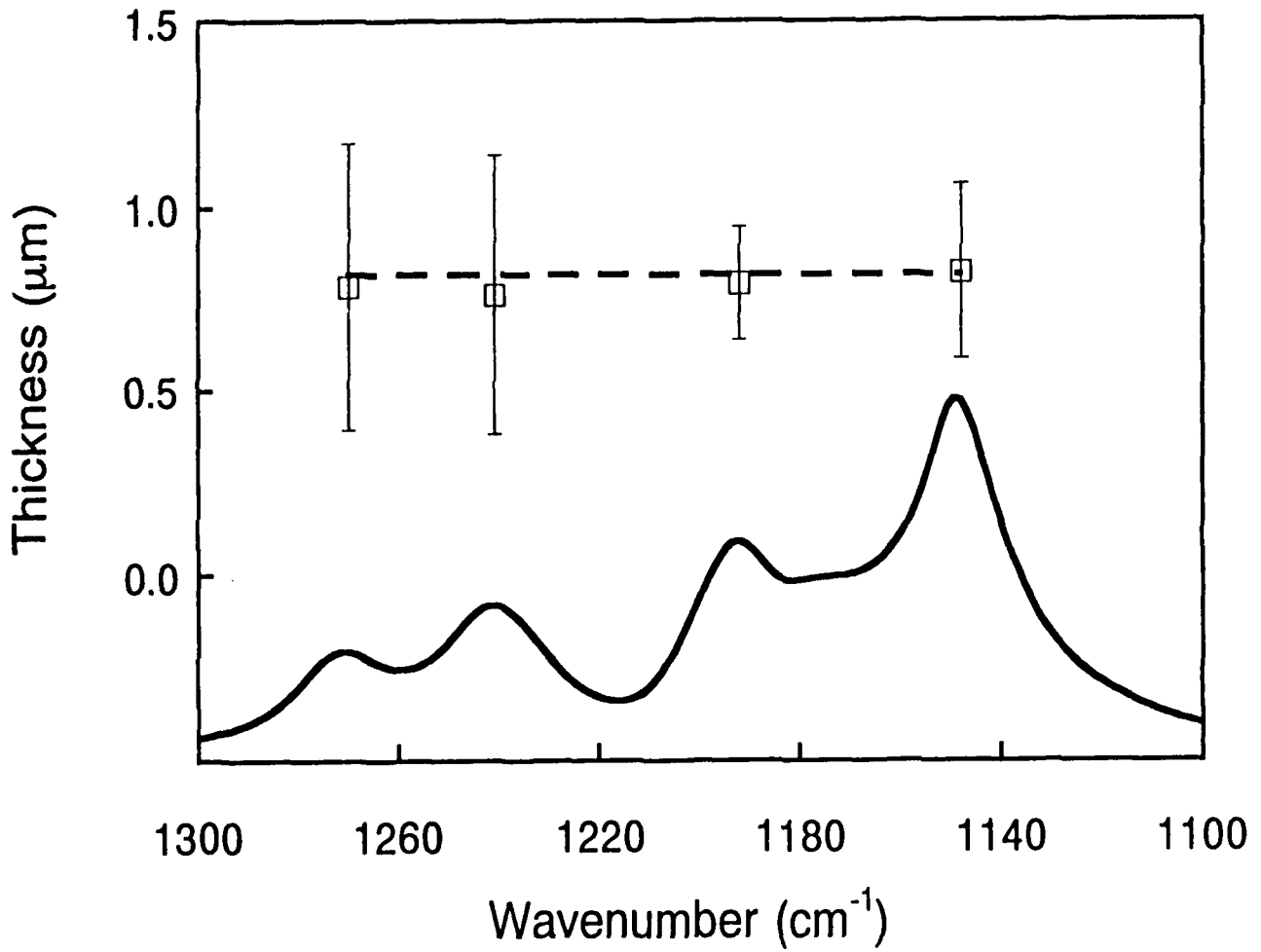
1.5
1.0
0.5
0.0
Thickness (μm)
1300
1260
1220
1180
1140
1100
Wavenumber (cm-1)

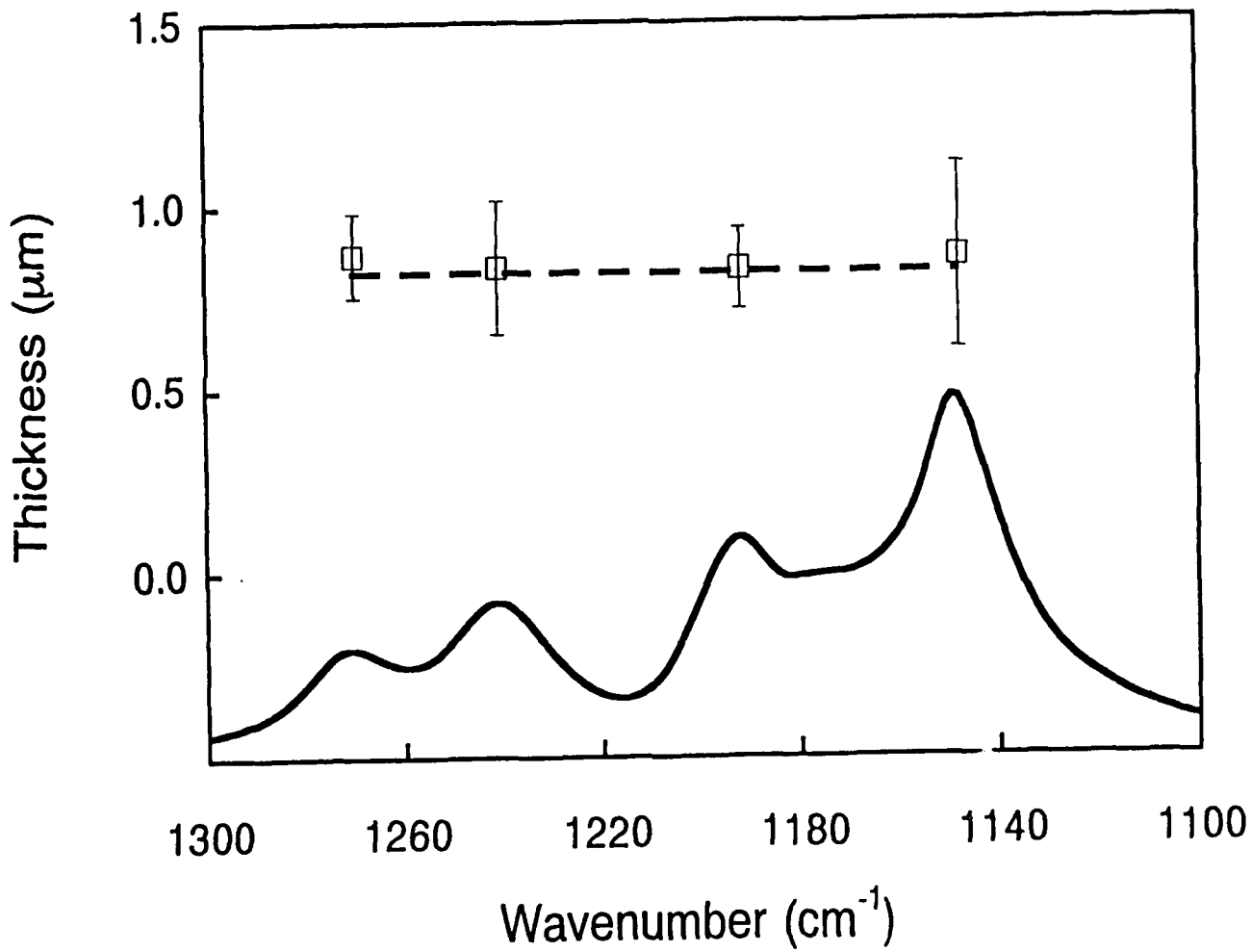
1.5
1.0
0.5
0.0
Thickness (μm)
1300
1260
1220
1180
1140
1100
Wavenumber (cm-1)

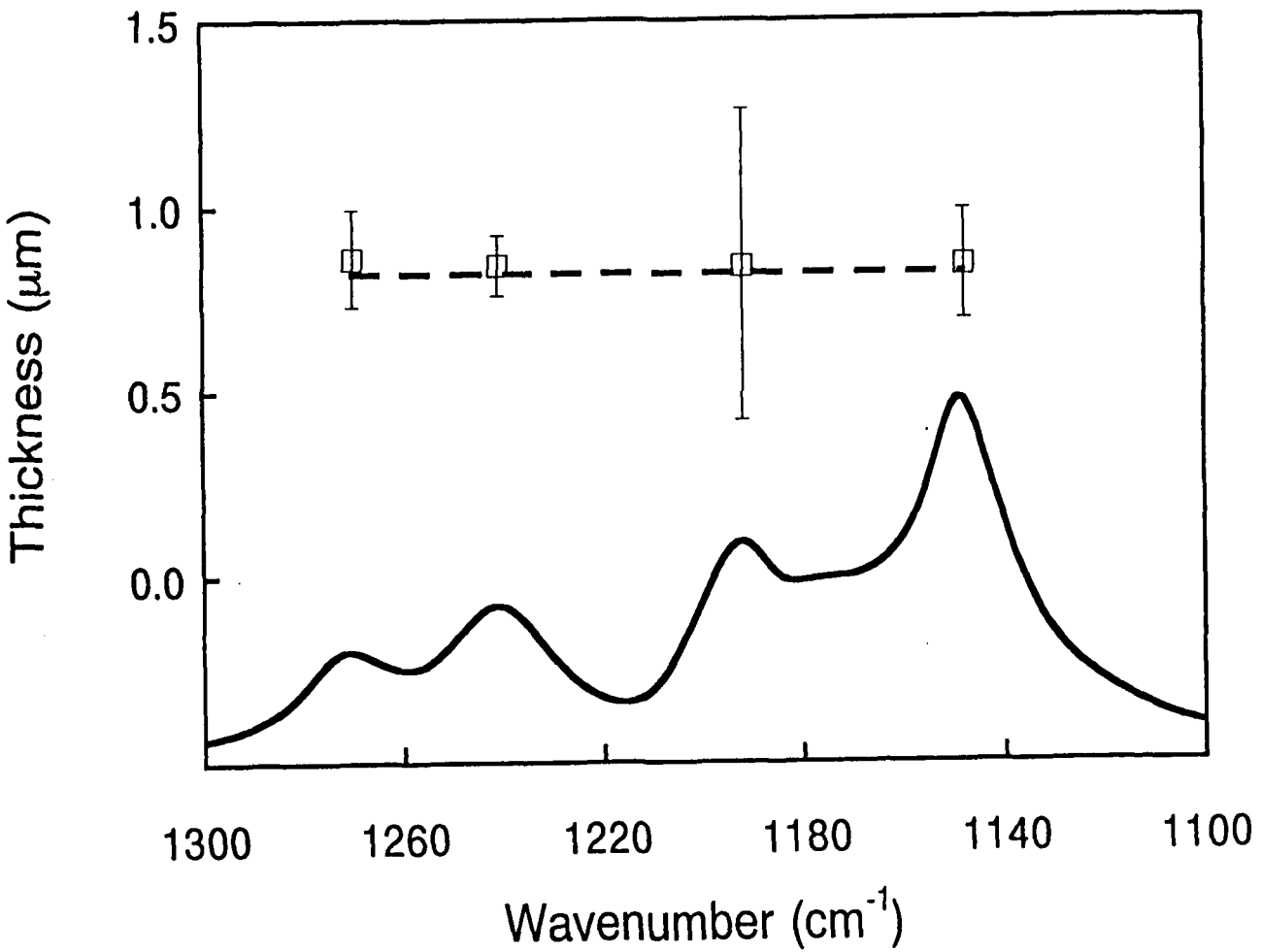

Shick et al Figure 12

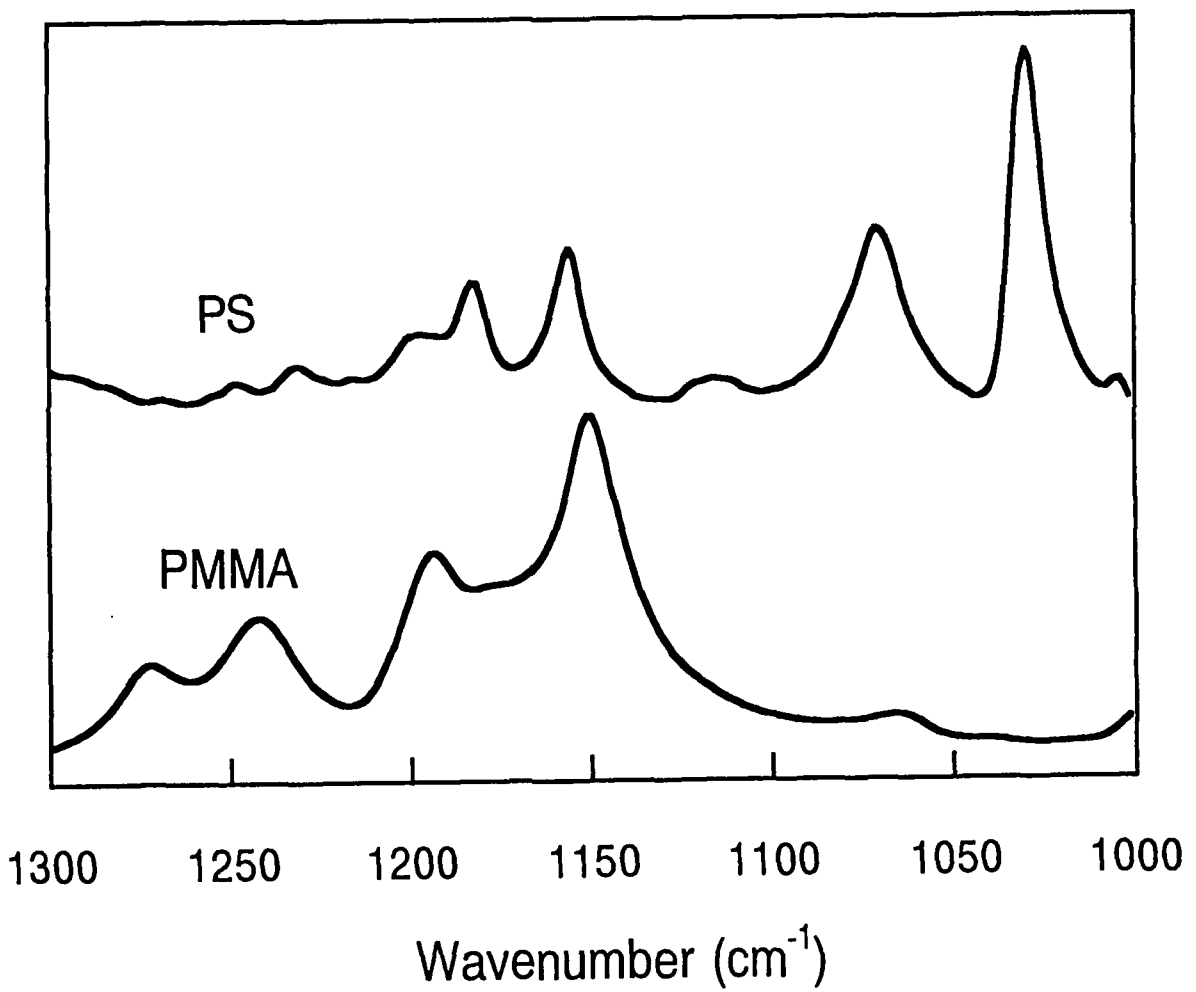
PS
PMMA
1300
1250
1200
1150
1100
1050
1000
Wavenumber (cm-1)

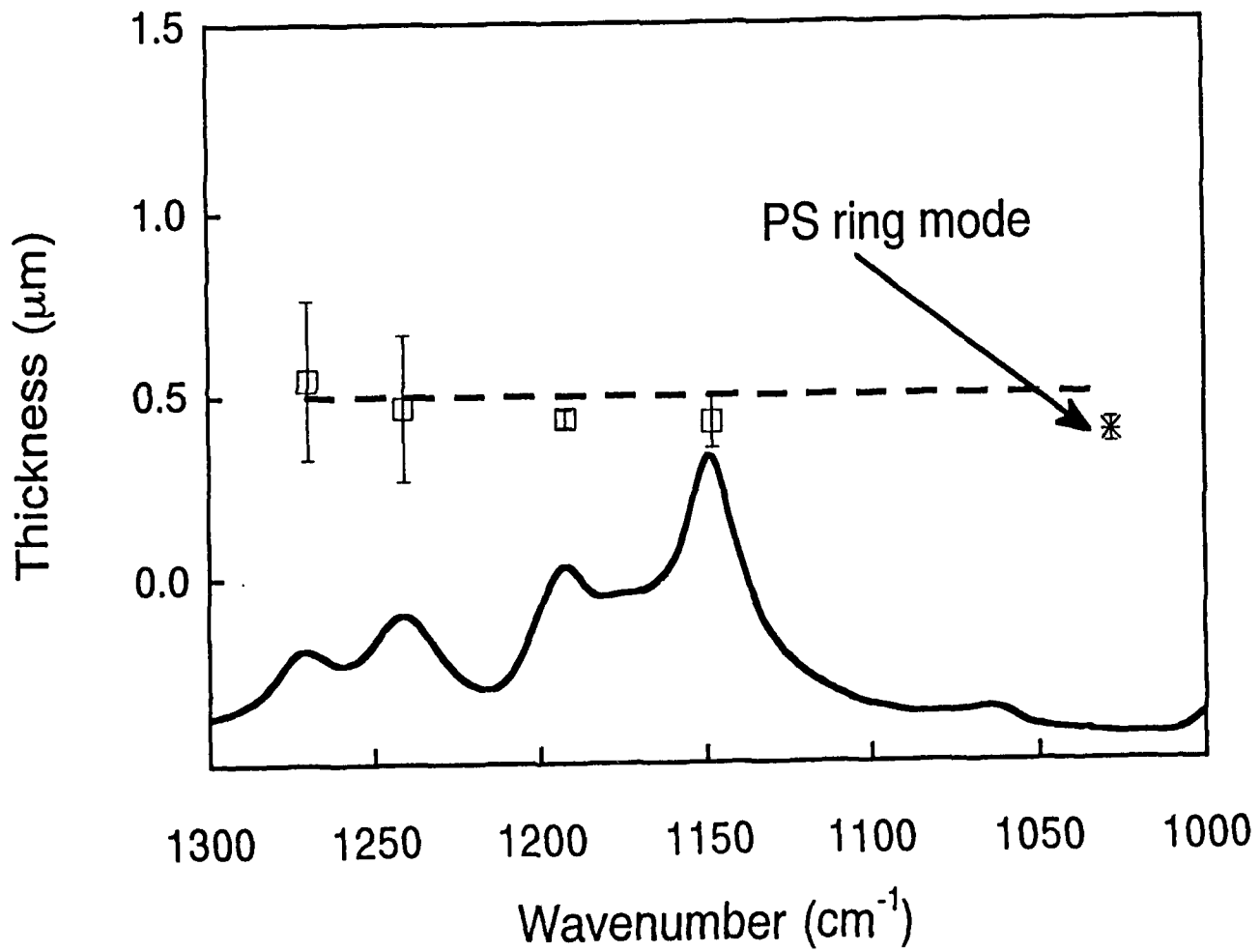
1.5
1.0
0.5
0.0
Thickness (μm)
PS ring mode
1300
1250
1200
1150
1100
1050
1000
Wavenumber (cm-1)

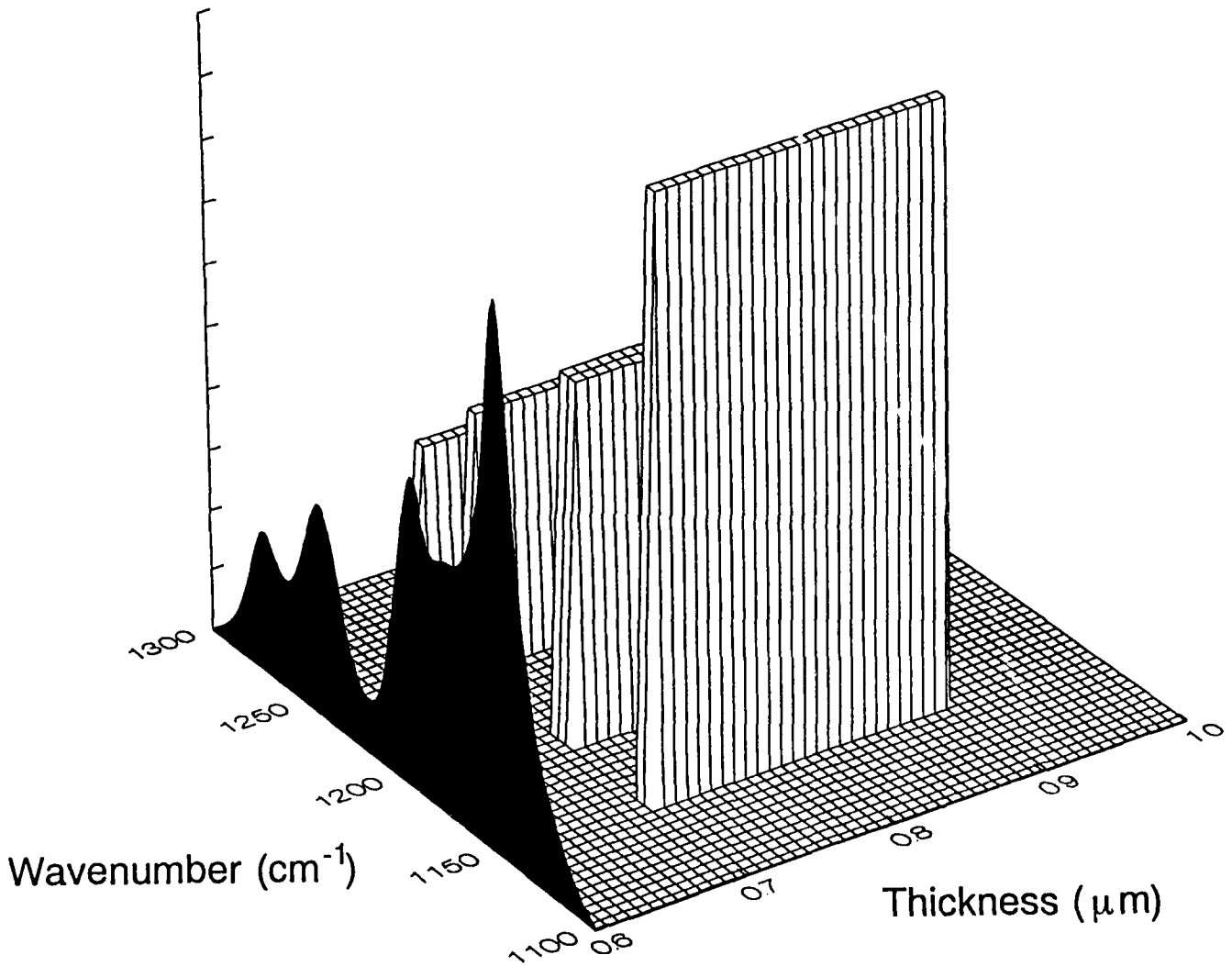
1300
1250
1200
1150
1100
Wavenumber (cm-1)
06
07
08
09
10
Thickness (μm)

Fig. 15